NUMERICAL STUDY OF ORGANIC RANKINE CYCLE RADIAL-INFLOW TURBINES FOR HEAVY-DUTY DIESEL ENGINE COOLANT HEAT RECOVERY

Lei Zhang[1], Weilin Zhuge[1], Yangjun Zhang[1]*, Jie Peng[2]

[1]State Key Laboratory of Automotive Safety and Energy, Tsinghua University, Beijing, 10084, China
zlei11@mails.tsinghua.edu.cn
zhugewl@tsinghua.edu.cn
yjzhang@tsinghua.edu.cn

[2]Department of Engineering Mechanics, Tsinghua University, Beijing, 10084, China
peng-jie@tsinghua.edu.cn

* Corresponding Author

ABSTRACT

Low rotating speed radial-inflow turbines are promising for the organic Rankine cycle systems in the small power size applications such as heavy-duty trucks and passenger cars waste heat recovery. Small mass flow rate and low rotating speed will lead to the turbine design specific speed lower than the optimal range of 0.34 to 0.72. Until now, few literatures reported the performance characteristics and loss mechanisms of low specific speed ORC radial-inflow turbines. The present study makes a RANS simulation of the low specific speed of 0.28 radial-inflow turbine using R245fa as working fluid to evaluate its performance characteristics and investigate the loss mechanisms. An optimal specific speed of 0.47 radial-inflow turbine in the same nominal operating condition and working fluid is also simulated for comparative analysis. The CFD results indicate that the low specific speed turbine nominal efficiency decreases 1.7% compared with the optimal one. And furthermore the off-design efficiency decreases are in the range of 2.6% to 0.6% from low to high pressure ratio conditions. The effect of specific speed on the efficiency characteristics mainly lies on rotor tip clearance and passage losses. The low specific speed turbine shows larger tip clearance losses but smaller passage losses compared with the optimal specific speed turbine. Flow field analysis of rotor entropy generation indicates that for the low specific speed turbine, the entropy generation caused by the tip clearance flow is much larger, and the tip clearance loss is mainly located on the suction surface in the inducer to midchord region, but on the pressure surface in the exducer region.

1. INTRODUCTION

More and more attention is being paid by the automobile research institutes and manufacturers to the organic Rankine cycle (ORC) power system, which can significantly improve the internal combustion engine efficiency by recovering the waste heat like exhaust gas and coolant. The use of organic fluids instead of water makes the power system suitable for low (below 230℃) to middle (230-650℃) temperature waste heat recovery. Furthermore, single stage expanders can satisfy the pressure ratio demand for most applications, and there exists no need of superheating and no risk of blades erosion when dry or isentropic type organic fluids are used (Tchanche *et al.*, 2011).

Radial-inflow turbines have been widely researched in the power size from 50 to 5000kW in the ORC system. However, when the power size is below 50kW or even 10kW with applications in the range of heavy-duty trucks to passenger cars it is not considered as a potential expander type compared with scroll expanders (Quoilin *et al.*, 2013). The high design rotating speed to satisfy the optimal specific speed of radial-inflow turbines is the main reason. Low specific speed radial-inflow turbines can be competitive in the small power size applications.

Specific speed, which is used extensively in studies of radial-inflow turbines, is a correlation between design features and efficiencies. **Figure 1** is the classic chart of the relationship between radial-inflow turbine specific speeds and losses documented by Rohlik (1968) based on various loss models. The results showed peak total-to-static efficiency of 87% close to dimensionless specific speed around 0.6, with efficiencies diminishing at lower and higher specific speed. The chart showed that the efficiency would drop to 80% when the specific speed was 0.3, and the efficiency would further drop to 70% when the specific speed was 0.15. The experimental research by Kofskey and Nusbaum (1972) also showed that a maximum peak total-to-static efficiency of 89% could be obtained at the specific speed of about 0.51. The efficiencies would be above 80% within the specific speed range of 0.34 to 0.72. There was a rapid decrease in efficiencies at both ends of the specific speed curve.

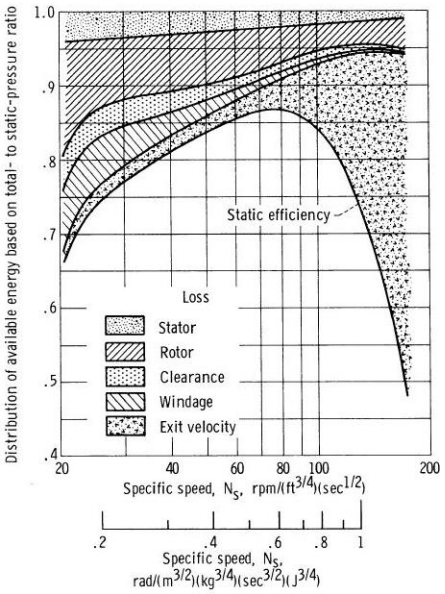

Figure 1: Prediction of radial-inflow turbine loss breakdown (Rohlik, 1968)

Numerical analysis of ORC turbine performance characteristics and loss mechanisms just starts in the recent five years. The mainly researched turbines still follow the basic principle, which is to select the design rotating speed to make the specific speed within the optimum range of 0.34 to 0.72. Li *et al.* (2011) studied a 3.8kW partial admission radial turbine with R11 as working fluid. The design specific speed was about 0.41, and the efficiency can only reach 62.5%. The authors depict the effects of partial admission on the flow field in the rotor passage. Some losses arise because of the mixing of high and low momentum fluid, interaction of some vortexes and vortexes dissipation. Cho *et al*. (2014) designed a partial admission impulse radial turbo-expander for 30kW application with specific speed of 0.39, and simulated the performance characteristics in two power size, 30kW and 3kW. The authors showed the results of optimal rotating speed and nozzles numbers under different inlet total temperatures. As for the turbine efficiency, it was shown that the partial admission rate had great influence, the value of which dropped from 77% to 62% in 30kW, and from 52% to 39% in 3kW as the partial admission rate decreased. Sauret and Gu (2014) studied a 400kW radial-inflow turbine with R143a as working fluid. The specific speed was 0.60, and the nominal total-to-static efficiency was 83.5%. And also large amount of off-design conditions were simulated to analyze its performance characteristics. The results showed that efficiencies would drop 10-20% when the rotating speed increased or decreased by 20%. Zhang *et al*. (2014) simulated a 10kW radial-inflow turbine with R123 as working fluid to discuss the real gas effects in the nozzle and rotor. The design specific speed was 0.58, and the nominal total-to-static efficiency was 83.5%. The authors mainly focused on the property differences between real and perfect gas model simulation results, thus the discussion about performance characteristics did not mentioned. Wheeler and Ong (2014) analyzed a 155kW shrouded radial-inflow turbine with pentane as working fluid. The design specific speed was 0.34, and the reported total-to-static efficiency was 85.8% without taking tip clearance loss into account. The authors demonstrated that as the Mach number in the nozzle outlet reached near 1.4, using the

constant height inducer would lead to relative flow acceleration and then high peak Mach number in the inducer. Through the inducer shape redesign, 1.3% efficiency improvement was obtained.
Since the mainly reported ORC radial-inflow turbines are designed within the optimum specific speed range, there exist few literatures relating to the performance characteristics analysis of low specific speed turbines. In the present work, three-dimensional steady RANS simulations were carried out to study the performance characteristics of 0.28 specific speed ORC radial-inflow turbine for heavy-duty diesel engine coolant heat recovery. Furthermore an optimal specific speed of 0.47 radial turbine is also simulated for comparative analysis. The paper was organized as following, the two specific speed turbines in the same nominal condition were preliminarily designed in section 2. And then, the numerical method and grid independence analysis were described Section 3. Section 4 proceeded with the comparative study of the performance characteristics of the low and optimal specific speed turbines and furthermore the discussion of loss mechanics, followed by the conclusions.

2. PRELIMINARY DESIGN

First of all, dimensionless parameters of specific speed n_s and blade-to-jet speed ratio ν are used to determine the rotating speed ω and rotor inlet radius r_4, which is also the radial-inflow turbine feature size. The definitions of these two parameters are,

$$n_s = \omega\sqrt{Q_6}/(h_{0,sg} - h_6)_{is}^{3/4} \tag{1}$$

$$\nu = \omega r_4/\sqrt{2(h_{0,sg} - h_6)_{is}} \tag{2}$$

Besides the specific speed n_s and blade-to-jet speed ratio ν, the preliminary design process cannot be completed until some other essential empirical parameters are determined. During the last several decades, the recommended values of these empirical parameters for perfect gas axial and radial turbine design developed a lot on the benefit of aero engine rapid development. Now it is an opportunity for the ORC turbine to rapidly develop on the benefit of organic Rankine cycle technologies promising future. However, as the lack of abundant design cases of the ORC turbine, it is preferred to utilize the recommended empirical values for perfect gas turbines in the ORC radial-inflow turbine preliminary design process. The essential eight empirical parameters and their recommended values are listed in **Table 1**. And the principal geometry parameters and locations of different subscript numbers are illustrated in **Figure 2**.

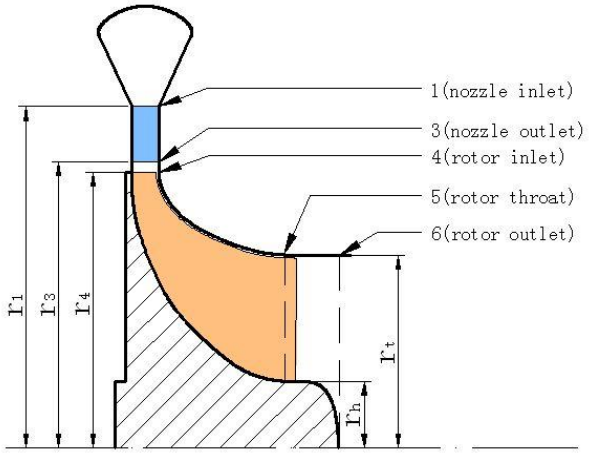

Figure 2: A diagram of radial-inflow turbine principal geometry parameters and locations

As few discussions about nozzle vane number determination, it is set to the number equal to the rotor blade number. Furthermore, the rotor blade numbers are the values calculated based on Glassman method minus three to avoid excessive blockage and high friction losses. The geometry design results of low and optimal specific speed ORC radial-inflow turbines are shown in **Table 2**.

Table 1: Empirical parameters and their recommended values in the preliminary design process

Empirical Parameter	Symbol	Recommended Values
Nozzle vane exit angle	α_{b3}	characterized by specific speed (Rohlik,1968)
Nozzle vane number	Z_n	few recommendations
Nozzle vane radius distance	r_1-r_3	0.4r$_4$ (Concepts NREC, 2014)
Interspace radius distance	r_3-r_4	2$b_3$cosα_3 (Watanabe *et al.*, 1971)
Rotor blade exit angle	β_{b6}	-55 (Whitfield, 1990)
Rotor blade number	Z_r	(π/30)(110-α_3)tanα_3 (Glassman, 1976)
Rotor exit tip to inlet radius ratio	$r_{6,t}/r_4$	characterized by specific speed (Rohlik,1968)
Rotor exit hub to tip radius ratio	$r_{6,h}/r_{6,t}$	0.35 (Zhang, 2013)

Table 2 : Preliminary design results of low and optimal specific speed ORC turbines

Component	Geometry Parameters	Low Specific Speed Turbine	Optimal Specific Speed Turbine
Dimensionless parameters	Specific speed	0.28	0.47
	Blade-to-jet speed ratio	0.70	0.70
Volute	Throat radius [mm]	129	85
	Throat area [mm^2]	1017	908
Nozzle	Inlet radius [mm]	100	62
	Inlet vane angle [°]	70	67
	Exit radius [mm]	84	52
	Exit vane angle [°]	80	77
	Number of vanes	15	12
Interspace	Exit radius [mm]	82.5	50
Rotor	Rotating speed [rpm]	15,000	25,000
	Inlet blade height [mm]	5	5
	Exit tip radius [mm]	50	35
	Exit hub radius [mm]	18	12
	Exit blade angle[°]	-55	-55
	Number of blades	15	12
	Tip clearance [mm]	0.3	0.3
Predicted performance	Mass flow rate [kg/s]	0.761	0.756
	Power [kW]	10.1	10.3
	Total-to-static efficiency	80.6%	83.0%

3. NUMERICAL METHOD

The steady state simulation of the ORC radial-inflow turbines designed in section 2 were carried out using the commercial CFD code FINE^{TM}/Turbo. FINE^{TM}/Turbo is a Reynolds-average Navier-Stokes equation solver that is based on the finite volume method, and uses 5 stage explicit Runge-Kutta scheme and multi-block structured meshing strategy (NUMECA, 2014). The turbulence model used in this calculation is the SST k-ω model.

The treatment of the real gas model for R245fa in this CFD code has been discussed in the former study (Zhang, 2014). Some setting parameters are modified. The Helmholtz energy equation of state (Lemmon and Span, 2006) fitted for organic fluid R245fa is utilized to calculate the gas properties. The available temperature is limited to the range of 273K to 433K, and available pressure is from 0.05MPa to 4.00MPa. The grid number of data tables are increased by 60%, and bicubic interpolation method replaced the bilinear interpolation method. The purpose of all these modifications is to improve accuracy of the datum used for evaluating R245fa properties in the CFD code.

The CFD domain consists of three components: the nozzle ring, the rotor wheel, and the exhaust pipe, shown in **Figure 3**. The domain was meshed using the multi-block structured tool AutoGrid5^{TM}. A fine mesh with 1,234,428 number of grid points was generated, which kept y^+ lower than 4 in the nozzle vane surfaces and 2 in the rotor blade surfaces. The distribution of the mesh was 175,263 grid points within the nozzle ring passage, 833,072 grid points within the rotor wheel passage and 226,093 grid points within the exhaust pipe passage. The grid independency study showed that the increase of grid

point number by 100% in each orthogonal grid direction only made a 0.2% difference in the predicted mass flow rate and 0.4% difference in the predicted torque. It indicated that the discretization error was reduced to an acceptable error in the current grid point number.
Total pressure and total temperature with velocity direction after the volute were used as the inlet boundary condition because the CFD domain did not include the volute. The values of inlet boundary conditions were obtained from the one-dimensional calculation results. The averaged static pressure was used as the exit boundary condition. All of the wall boundaries were treated as smooth and adiabatic. Another important consideration is the interface between the rotating and stationary domain. The "Mixing Plane" method using Conservative Coupling by Pitchwise Row scheme was adopted.

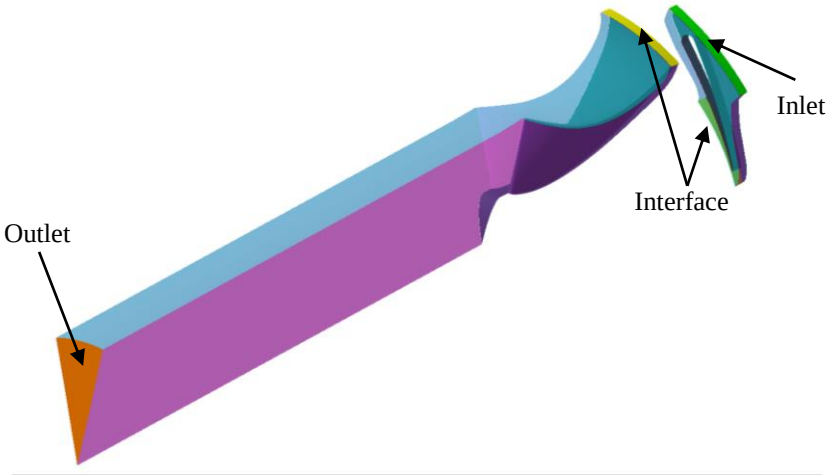

Figure 3: CFD domain of the radial turbine

4. RESULTS AND DISCUSSIONS

In this section, the CFD simulation results are analyzed. Firstly, the performance characteristics of low and optimal specific speed turbines are compared. And then six loss models are used to break down the losses based on the CFD datum to explain the influence of specific speed on efficiency differences. Finally, the flow field comparisons of rotor entropy generation between low and optimal specific speed turbines are carried out to discuss the loss mechanisms.

4.1 Turbine Performance Characteristics

Mass flow rate and efficiency are the two main performance parameters for turbines. In general, the reduced mass flow rate $\dot{m_{rd}}$ and total-to-static isentropic efficiency η_{ts} are used for the radial-inflow turbine performance description. The definitions of these two performance parameters are,

$$\dot{m_{rd}} = \frac{\dot{m}\sqrt{T_{0,sg}}}{p_{0,sg}} \tag{3}$$

$$\eta_{ts} = \frac{P}{\dot{m}(h_{0,sg}-h_{6})_{is}} \tag{4}$$

Figure 4 and **Figure 5** show the performance characteristics of the low and optimal specific speed turbines. Three rotating speed lines besides the design rotating speed line were simulated, the values of which were set to 0.7, 0.85 and 1.15 times of the design rotating speed. The calculated pressure ratios were in the range of 2.0 to 4.5. As is shown in **Figure 4(a)** and **Figure 5(a)**, when the pressure ratio is above 3.0, the turbine is choked. In this pressure ratio range (above 3.0), the reduced mass flow rate only has relationship with the pressure ratio, and it changes a little as the pressure ratio increases. However, in the low pressure ratio range (below 3.0), the mass flow rate has relationship with the pressure ratio and rotating speed, and it changes a lot based on the pressure ratio. The reduced mass flow rate is determined by nozzle throat area. As the throat area is the same for the two

turbines, the difference of chocked reduced mass flow rate is within 1% for the low and optimal specific speed turbines.

As for the total-to-static isentropic efficiency shown in **Figure 4(b)** and **Figure 5(b)**, the nominal efficiency of low specific speed turbine is 1.7% lower than that of the optimal specific speed turbine. The off-design operating conditions mainly locate in the envelope line of the efficiency curves. For the low specific speed turbine, the total-to-static efficiencies change in the range of 79.5% to 83.3% when the pressure ratios increase from 2.0 to 4.5. For the optimal specific speed turbine, it is obvious that higher efficiencies can be achieved in the envelope line. The maximum improvement of 2.6% occurred in the condition of pressure ratio equal to 2.0, and the minimum improvement of 0.6% occurred in the condition of pressure ratio equal to 4.0. In addition, for the off-design operating conditions, which are below the efficiency envelope line, the specific speed also has great influence. For the operating conditions, where the rotating speed is high and the pressure ratio is low, the efficiencies of low specific speed turbine is 7-9% lower; for the operating conditions, where the rotating speed is low and the pressure ratio is high, but in contrary the efficiencies of low specific speed turbine is slightly higher. It indicates that the specific speed has great influence on the turbine nominal and off-design efficiencies, especially on the operating conditions that pressure ratio is lower than the design value.

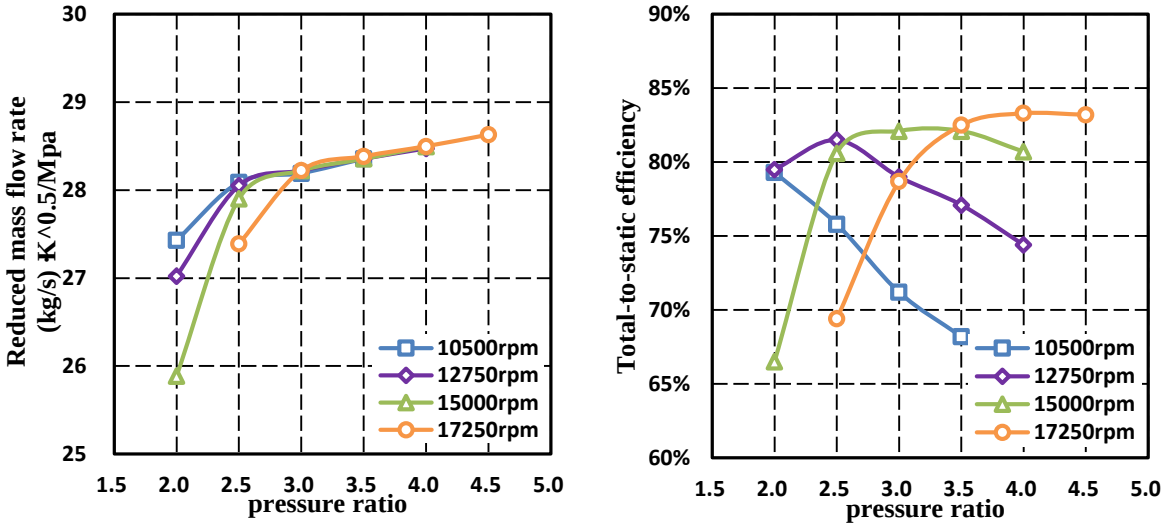

(a) (b)

Figure 4: Performance characteristics of the low specific speed turbine

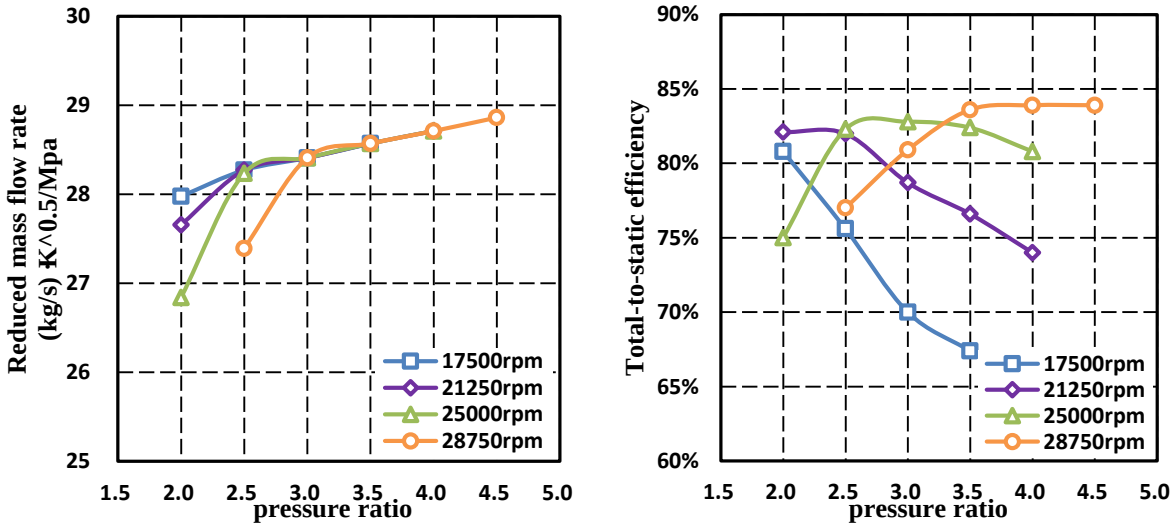

(a) (b)

Figure 5: Performance characteristics of the optimal specific speed turbine

4.2 Breakdown of Losses

The breakdown of losses can illustrate that which component has the greatest influence on the efficiency dropping. A way to divide losses in a radial-inflow turbine stage was documented by Rohlik (1968), he divided them into stator loss, rotor loss, clearance loss, windage loss and exit velocity loss. In the present study, based on the authors' experience, the radial-inflow turbine stage loss is divided into stator loss, inlet incidence loss, rotor passage loss, trailing edge loss, tip clearance loss, and exit velocity loss (seen in **Figure 6**). Each loss is represented by a mathematic model which has some basis in the turbine physical processes. The windage loss is not taken into consideration.

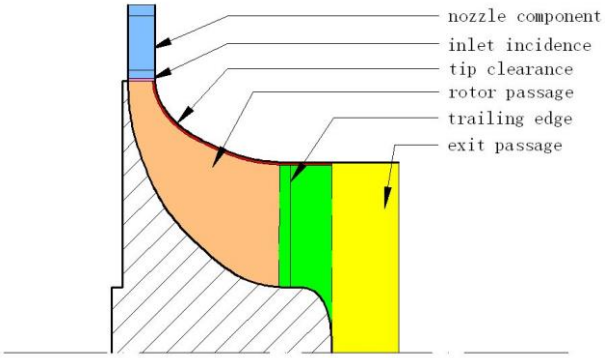

Figure 6: Division of the radial-inflow turbine stage for analysis of loss distribution

The nozzle loss model was developed by Rodgers (1987). It was based on Rodgers' own test data and the Ricardo data. A static enthalpy loss coefficient ξ_n was proposed based on the nozzle exit Reynolds number Re_3, nozzle blade solidity, and throat aspect ratio,

$$\xi_n = \frac{h_3 - h_{3,is}}{h_{3,sg} - h_3} = \frac{0.05}{\mathrm{Re}_3^{0.2}}\left(\frac{3\tan\alpha_{b3}}{s/c} + \frac{o}{b_3}\right) \tag{5}$$

where $Re_3 = \rho_3 C_3 b_3 / \mu_3$.

The inlet incidence loss L_i refers to any work of the organic fluid turning from its direction of approach to the rotor to the direction required by the blade passage. The incidence loss is the contribution to the entropy generated, when the turbine is operating away from its design point and the rotor inlet flow angle is not equal to its optimum $\beta_{4,opt}$ (Wasserbauer and Glassman, 1975).

$$L_i = \frac{1}{2} W_4^2 \sin^2(\beta_4 - \beta_{4,opt}) \tag{6}$$

where $\beta_{4,opt} = 10°$.

The rotor passage loss L_p includes the losses due to cross-stream or secondary flows, the mixing which these bring about, and the blockage and loss of kinetic energy due to the growth of boundary layers. The rotor passage loss formulation based on the mean kinetic energy of the fluid in the blade passage are widely used, and its developed form by Wasserbauer and Glassman (1975) is based on the meridional component of kinetic energy at inlet but the whole kinetic energy at the rotor throat.

$$L_p = \frac{1}{2} K_p \left(W_4^2 \cos^2\left(\beta_4 - \beta_{4,opt}\right) + W_5^2\right) \tag{7}$$

where K_p is an empirical coefficient, for which a value of 0.3 is recommended.

The rotor passage loss formulation applies between the inlet and throat of the rotor, and the trailing edge loss L_{trl} is modeled between the throat and rotor outlet. The tangential component of absolute velocity is assumed to be constant, and a trailing edge loss is based on a sudden expansion from the rotor throat to an area just downstream of the rotor outlet (Moustapha *et al.*, 2003).

$$L_{trl} = \frac{1}{2}\left(C_{5,m} - C_{6,m}\right)^2 \tag{8}$$

The tip clearance loss L_{clr} refers to the leakage flow through the gap between the tip and shroud. The leakage flow can be written in terms of separate leakage gaps in the axial, radial and cross-coupling portions (Dambach *et al.*, 1998).

$$L_{clr} = \frac{U_4^3 Z_r}{8\pi}(K_a \varepsilon_a C_a + K_r \varepsilon_r C_r + K_c \sqrt{\varepsilon_a \varepsilon_r C_a C_r}) \quad (9)$$

where $C_a = \frac{1-(r_{6,t}/r_4)}{C_{4,m} b_4}$ and $C_r = (\frac{r_{6,t}}{r_4}) \frac{z-b_4}{C_{6,m} r_6 b_6}$. And K_a, K_r and K_c are the discharge coefficients for the axial, radial and cross-coupling portions of the tip gap respectively. Good agreement with test data was achieved with $K_a = 0.4$, $K_r = 0.75$ and $K_c = 0.3$.

The exit velocity loss L_e relates to the exit absolute velocity of the organic fluid which cannot be used.

$$L_e = \frac{1}{2} C_6^2 \quad (10)$$

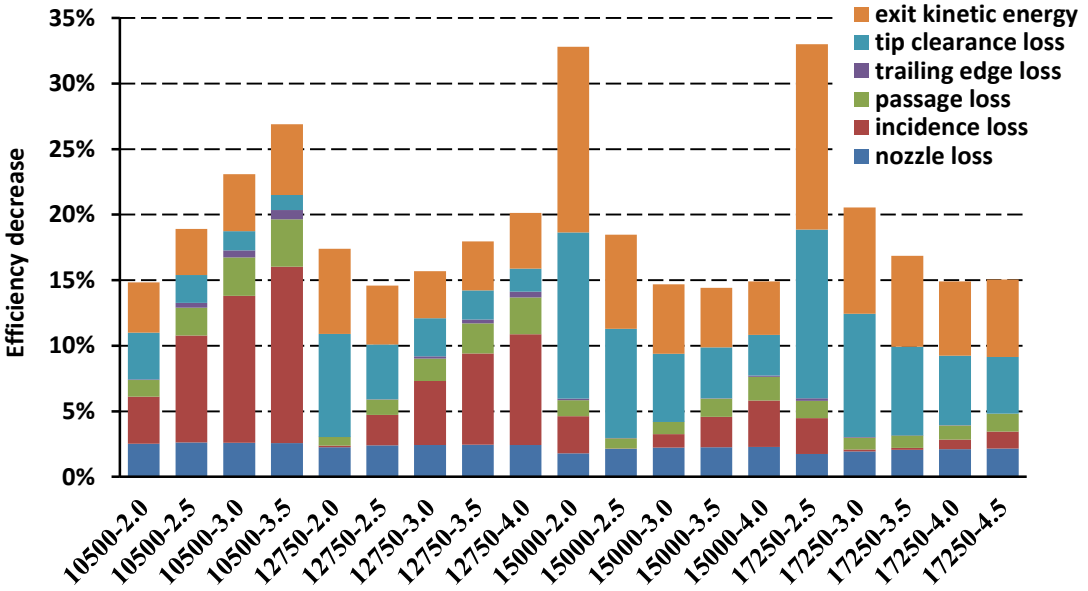

(a) Low specific speed turbine

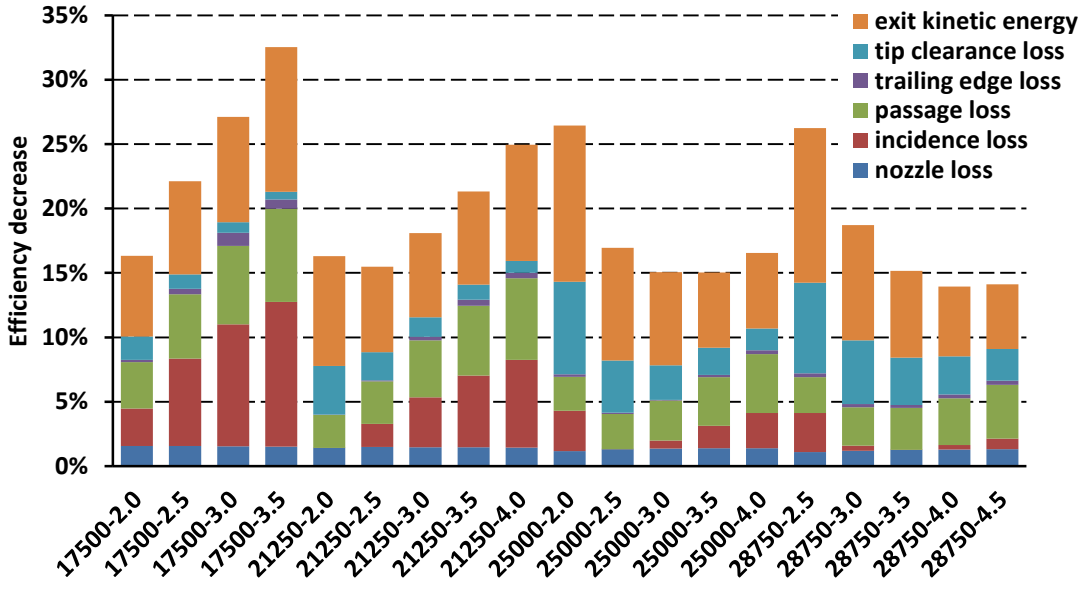

(b) Optimal specific speed turbine

Figure 7: Breakdown of losses for the low and optimal specific speed turbines

Figure 7 shows the breakdown of losses for the low and optimal specific speed turbines. Each column is a specific operating condition, where the first number represents the rotating speed and the second one is the pressure ratio. In general, compared with rotor losses, the stator losses are much smaller in all the operating conditions of the two turbines. The losses related to the rotor dominate the turbine efficiency dropping, except the high rotating speed with low pressure ratio operating conditions, where the exit velocity losses are dramatically large. For the high rotating speed with low pressure ratio conditions, the exit kinetic energy losses are much larger than the average values of all the operating conditions, and also the tip clearance losses are larger than the average values. Both of these two losses make the efficiency drop a lot. What's more, as the tip clearance losses of low specific speed turbine increase much larger, the efficiencies of low specific speed turbine in these conditions are much lower than those of optimum specific speed turbine.

When comparing the loss distributions related to rotor between low and optimal specific speed turbines, it leads to the following results. The low specific speed turbine shows larger tip clearance losses but smaller passage losses compared with the optimal specific speed turbine; the trailing edge losses are much smaller compared with other losses; incidence losses are determined by the operating conditions. For low rotating speed with high pressure ratio operating conditions, incidence losses are very large, even can dominate the rotor loss in some extreme operating conditions. It is mainly caused by the very large positive incidence angles. What's more, low specific speed turbine show smaller exit kinetic velocity losses in these conditions, which lead to a slight improve of the efficiencies. For the operating conditions located in the efficiency envelope line, the incidence losses are much smaller, and the losses are dominated by the tip clearance loss and rotor passage loss.

A typical operating condition in the efficiency envelope line is the nominal operating condition. For the nominal operating condition, the tip clearance loss of low specific speed turbine can be as much as above 8% accounting for more than 40% of the total loss, but the tip clearance loss of optimal one is only 4%. However, the passage loss of low specific speed turbine is only 0.8% compared with 2.7% of the optimal specific speed turbine. The similar situation occurred for the off-design point located in the efficiency envelope line. On the one hand, these differences can be explained by the differences of geometry parameters in **Table 2**. The low specific speed design will lead to larger geometry size for the same design power output. Furthermore, it will lead to smaller magnitude of velocity parameters but larger values of parameters related to tip clearance. Hence, it would decrease the passage losses but increase the tip clearance losses. On the other hand, the efficiency differences can be better explained when the flow field of rotor entropy generation is well understood.

4.3 Rotor Entropy Generation

The rotor flow field comparison in the nominal condition is carried out to discuss the influence of specific speed on the entropy generation in the rotor tip clearance and passage. As described in the tip clearance loss model, the tip clearance loss is mainly caused by the fluid moving from pressure surface (PS) to the suction surface (SS) of the blades. The kinetic energy carried by the fluid is dissipated into the main flow, and at the same time it may enhance the vorticity in the rotor passage, which will further increase the loss. From the research by Dambach et al. (1998), the tip clearance flow in a radial-inflow turbine can be divided into three regions, inducer, midchord, and exducer. The flow field of vorticity and entropy in these three regions are shown in **Figure 8** and **Figure 9**.

Compared with the optimum specific speed turbine, **Figure 8(a)** illustrates that in the inducer region larger contribution of entropy generation is caused by the tip clearance on the suction surface, and the scrapping effect caused by relative casing motion is also stronger to increase the passage loss. In the midchord region shown in **Figure 8(b)**, tip clearance also makes larger contribution of entropy generation on the suction surface, and further the vortex is generated by the tip clearance flow. Although complicated rotor passage vortexes are shown in **Figure 8(b)**, it seems that the vortex caused by the stronger scrapping effect in **Figure 9(b)** causes larger rotor passage loss compared with the low specific speed turbine. **Figure 8(c)** and **Figure 9(c)** illustrate that in the exducer region, the entropy generation caused by the tip clearance moves from suction surface to pressure surface. And a large vortex dominates the contribution of passage entropy generation for both of low and optimum specific speed turbines. To summarize, for the low specific speed turbine, much larger entropy generation is caused by the tip clearance flow, which is consistent with the results of loss model analysis, and flow field analysis of entropy generation indicates that the tip clearance loss is located on the suction

surface in the inducer to midchord region, but on the pressure surface in the exducer region. Further analysis of tip clearance flow may be an important aspect to improve the low specific speed turbine efficiency.

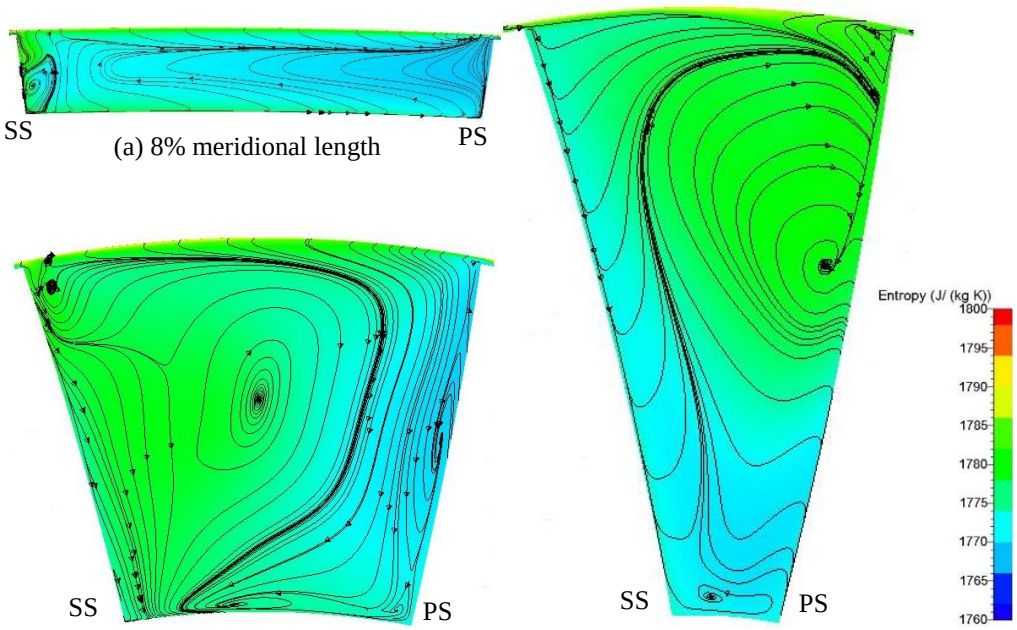

Figure 8: Vorticity and entropy on cross sections of the low specific speed turbine in the nominal condition

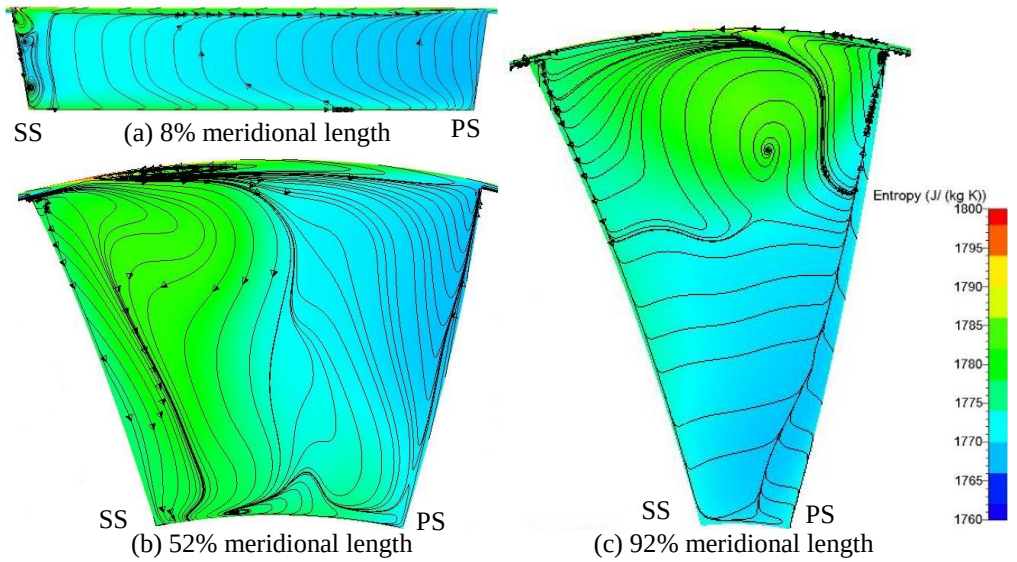

Figure 9: Vorticity and entropy on cross sections of the optimal specific speed turbine in the nominal condition

5. CONCLUSIONS

In the present study, three-dimensional steady RANS simulations have been carried out to investigate the performance characteristics and loss mechanisms of the ORC radial-inflow turbine using R245fa as working fluid applied for heavy-duty diesel engine coolant heat recovery. The comparison of performance characteristics and flow fields between low and optimal specific speed turbines has been analyzed. The results from this work suggest the following conclusions.

- When comparing the turbine performance characteristics between design specific speed of 0.28 and 0.47, the low specific speed turbine nominal efficiency decreases 1.7%. And furthermore in the efficiency envelope curve, the efficiency decreases are in the range of 2.6%

to 0.6% from low to high pressure ratio conditions. It indicates that the specific speed has great influence on the turbine nominal and off-design efficiencies, especially in the low pressure ratio conditions.

- The breakdown of losses indicates that the effect of specific speed on the performance characteristics mainly lies on rotor tip clearance and passage losses. The low specific speed turbine shows larger tip clearance losses but smaller passage losses.
- Flow field analysis of rotor entropy generation indicates that for the low specific speed turbine, much larger entropy generation is caused by the tip clearance flow, which is consistent with the results of loss model analysis, and furthermore the tip clearance loss is mainly located on the suction surface in the inducer to midchord region, but on the pressure surface in the exducer region.

In the future, a further study on the tip clearance flow in the low specific speed turbine rotor will be carried out to find out a flow control method to improve efficiencies of this kind of turbines.

NOMENCLATURE

C	absolute velocity	(m/s)
P	output power	(kW)
Q	volute flow rate	(m^3/s)
T	temperature	(K)
U	rotating velocity	(m/s)
W	relative velocity	(m/s)
Z_n	nozzle vane number	
Z_r	rotor blade number	
b	blade height	(m)
c	stator vane chord	(m)
h	enthalpy	(J/kg)
$\dot{m}$	mass flow rate	(kg/s)
o	stator throat opening	(m)
p	pressure	(Mpa)
r	radius	(m)
s	stator spacing	(m)
z	turbine axial length	(m)
α	absolute flow angle	(°)
α_b	nozzle vane angle	(°)
β	relative flow angle	(°)
β_b	rotor blade angle	(°)
ε	tip clearance	(m)
μ	viscosity	(Pa s)
ρ	density	(kg/m^3)
ω	rotating speed	(rad/s)

Subscript

0	volute inlet position
1	nozzle inlet position
3	nozzle outlet position
4	rotor inlet position
5	rotor throat position
6	rotor outlet position
a	axial direction
h	rotor hub position
is	isentropic process
m	meridian component
r	radial direction

sg	stagnation condition
t	rotor tip position

REFERENCES

Cho S.Y., Cho C.H., Ahn K.Y., Lee Y.D., 2014, A study of the optimal operating conditions in the organic Rankine cycle using a turbo-expander for fluctuations of the available thermal energy, Energy, 64:900-911.

Concepts NREC, 2014, Rital 8.3 Help.

Dambach R., Hodson H.P., Huntsman I., 1998, An experimental study of tip clearance flow in radial inflow turbines, ASME Paper No. 98-GT-467.

Glassman A.J., 1976, Computer program for design and analysis of radial inflow turbines, NASA Technical Note TN D-8164.

Kofskey M.G., Nusbaum W.J., 1972, Effects of specific speed on experimental performance of a radial-inflow turbine, Tech. rep., NASA Technical Note TN D-6605.

Lemmon E.W., Span R., 2006, Short Fundamental Equations of State for 20 Industrial Fluids, J. Chem. Eng. Data, 51, 785-850.

Li P., Chen J.H., Zhang D., Xie Y.H., 2011, Study on the steady and unsteady aerodynamic performance of a radial inflow turbine with small partial admission in a miniature ORC system, Proceedings of the ASME 2011 Power Conference.

Mousapha H., Zelesky M.F., Baines N.C., Japikse D., 2003, Axial and Radial Turbines, Concepts NREC, USA.

NUMECA, 2014, FINE™/Turbo v9.1 Theoretical Manual.

Quoilin S., Broek M., Declaye S., Dewallef P., Lemort V., 2013, Techno-economic survey of Organic Rankine Cycle (ORC) systems, Renewable and Sustainable Energy Reviews, 22:168-186.

Rodgers C., 1987, Mainline performance prediction for radial inflow turbines, Tech. rep., VKI Lecture Series.

Rohlik H. E., 1968, Analytical determination of radial inflow turbine design geometry for maximum efficiency, Tech. rep., NASA Technical Note TN D-4384.

Sauret E., Gu Y.T., 2014, Three-dimensional off-design numerical analysis of an organic Rankine cycle radial-inflow turbine, Applied Energy, 135:202-211.

Tchanche B.F., Lambrinos G., Frangoudakis A., Papadakis G., 2011, Low-grade heat conversion into power using organic Rankine cycles – A review of various applications, Renewable and Sustainable Energy Reviews, 15:3963-79.

Wasserbauer C.A., Glassman A.J., 1975, FORTRAN program for predicting the off-design performance of radial inflow turbines, NASA Technical Note TN D-8063.

Watanabe I., Ariga I., Mashimo T., 1971, Effects of dimensional parameters of impellers on performance characteristics of a radial inflow turbines, Trans ASME *Journal of Engineering for Power*, 93:81-102.

Wheeler A., Ong J., 2014, A study of the three-dimensional unsteady real-gas flows within a transonic ORC turbine, Proceedings of ASME Turbo Expo 2014.

Whitfield A., 1990, The preliminary design of radial inflow turbines, Trans ASME *Journal of Turbomachinery*, 112:50-57.

Zhang L., Zhuge W.L., Peng J., Liu S.J., Zhang Y.J., 2013, Optimization of the blade trailing edge geometric parameters for a small scale ORC turbine, IOP Conf. Series: Materials Science and Engineering 52(2013) 042016.

Zhang L., Zhuge W.L., Zhang Y.J., Peng J., 2014, The influence of real gas effects on ICE-ORC turbine flow field, Proceedings of ASME Turbo Expo 2014.

ACKNOWLEDGEMENT

The authors would like to thank the National Basic Research Program of China (2011CB707204) for the support.